Study on global dynamics of a special symmetrically laid composite laminated rectangular plate

Wensai Ma[1,*], Dongxiao Li[1], Fanghao Liu[1], Shufeng Lv[1]

[1]*Department of Mechanics, Inner Mongolia University of Technology, Hohhot, People's Republic of China*
**Correspondence author. Email: wensaima@163.com, ORCID: 0000-0001-9469-5605*

ABSTRACT

The global bifurcation and chaotic dynamics of the symmetrically laid orthotropic composite rectangular laminated plate on four simply supported sides is investigated for the first time by means of making use of the generalized Melnikov method. By utilizing the coordinate transformation theory to obtain the nonlinear dynamic system in five dimensions of composite laminated rectangular plates. Calculating the k-pulse Melnikov function of the system based on the generalized Melnikov theory so as to obtain the interval of the chaotic threshold for the composite laminated rectangular plate system. The numerical simulations are performed to validate the theoretical results by making use of MATLAB software, in order to come by bifurcation diagrams, phase diagrams and time history charts for composite laminated rectangular plates and identify the validity of the theoretical analysis. Finally, theoretical analysis and numerical simulation further demonstrate the existence of multi-pulse chaotic motion in composite laminated rectangular plates.

Key words: *Composite laminated rectangular plate; bifurcation; chaos; Melnikov method.*

1. INTRUCTION

Composite materials are favoured by an increasing number of researchers owing to their unique mechanical and electrical coupling, high specific strength, high specific stiffness and fatigue resistance [1-3], as a result of composite materials are usually thin-walled structures, and they are susceptible to undergo significant deformations under a great variety of external loads, making for complex geometric nonlinear dynamic characteristics. The nonlinear dynamic properties of composite material structures often result in the material structural destruction. Therefore, investigating ways to reduce or avoid the damage caused by nonlinear vibration in composite materials and make them play a maximum role in practical engineering and scientific applications is a highly meaningful research. Zhang et al. [4] analysed the nonlinear dynamics about an expanded orthotropic composite rectangular cantilever plate under the combined action of harmonic excitation in the flat surface and aerodynamic pressure. Yang et al. [5] utilized a multi-scale method for investigating the subharmonic resonance of a truncated conical shell of functionally gradient composites under the combined action of aerodynamic pressure and excitation within a two-dimensional plane. Ma et al. [6] discussed the nonlinear subharmonic resonance of the orthogonal anisotropic composite laminated rectangular plate. Noroozi and Bakhtiari-Nejad [7] studied the nonlinear dynamics and vibration characteristics of a composite cantilevered trapezoidal plates reinforced with carbon nanotubes for micro-aircraft, and examined the impact of plate geometric shape, volume fraction in carbon nanotubes, various excitation modes and other variables on the laminated

U. Vandandoo et al. (eds.), *Proceedings of the International Conference on Applied Sciences and Engineering (ICASE 2023)*,
Atlantis Highlights in Engineering 22,
https://doi.org/10.2991/978-94-6463-330-6_3

plate nonlinear vibration. Based on the first order shear deformation theory. Yang et al.[8] established a dynamic model for the laminated cylindrical shell with eccentric rotating carbon fiber reinforced polymer (CFRP), and studied the behaviour of the eccentric rotating CFRP laminated cylindrical shell under axial excitation with respect to buckling and free vibration. Yang et al.[9] investigated the buckling analysis and free vibration of a composite cylindrical shell reinforced with functionally gradient graphene sheet under axial excitation. Wu et al. [10] examined the nonlinear vibration behaviour of asymmetric composite laminated flat shells with bistable characteristics under fundamental excitation by theory and experiment.

In actuality, the mathematical models for the majority of engineering issues can be represented using high-dimensional nonlinear dynamics models. The dynamic behaviour exhibited high dimensional systems of nonlinear dynamics is exceptionally complex. It's precisely because of these complex dynamic behaviours in the system that the systemic material structure is often destroyed. Therefore, studying these complex dynamics behaviours in high-dimensional nonlinear dynamical systems, such as bifurcation, chaos and other complex dynamics, is of significant importance for the advancement of high dimensional nonlinear theory and the practical applications of engineering.

Zhang et al.[11] implemented the Melnikov method to examine the chaotic dynamics with multiple pulses of symmetrically laid simply supported composite materials under withstand the joint action of parametric excitation and extrinsic incentive. By using Melnikov's method, Zhang et al.[12] examined the chaotic dynamics and multi-pulse homologous orbit of a symmetrically laid orthogonal composite laminated cantilever rectangular plate under 1:1 internal resonance conditions. Zhu et al.[13] developed the high-dimensional Melnikov method, a tool suitable for studying parametric nonlinear dynamic systems with multi-periodic bifurcations, and applied the developed high-dimensional Melnikov method to research the multi-periodic motion of honeycomb sandwich composite laminates featuring a negative Poisson's ratio. The global bifurcation and chaotic dynamics of orthotropic composite laminated rectangular plates with four-sided simply supported symmetric laying under the action of external F_1 are investigated using the generalized Melnikov method in this article, and the theoretical analytical correctness is confirmed by numerical simulation method. Ma et al.[14] modified the generalized Melnikov method [15] for high dimensional systems and applied it to the study of complex nonlinear dynamic behaviours such as chaotic motion of annular antenna structures.

2. MECHANICAL MODEL

The mechanical model of symmetrically laid orthotropic composite laminated rectangular plates with four-sided simple supports is represented in Fig. 1. It is assumed that the rectangular plate length and width, as well as the composite laminated plate thickness, are denoted as a, b and h, and apply uniformly distributed harmonic excitation on the transverse plane with the equation $q = q_0 \cos \Omega t$, where q_0 is the amplitude of the excitation. The mechanical model of the discrete simply supported symmetrically laid orthotropic composite laminated rectangular plate with four sides is simplified as a two degrees of freedom ordinary differential system [6].

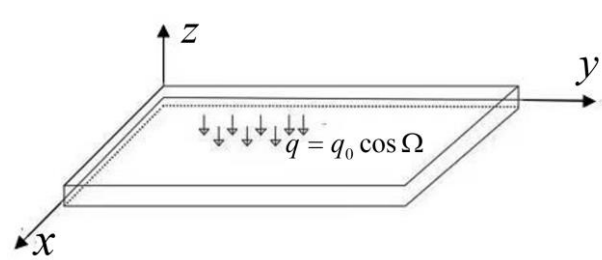

(a) Model and coordinate system

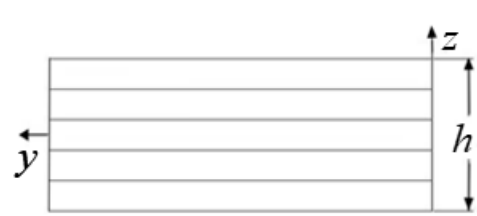

(b) Diagram of layer number distribution

Figure 1 Mechanical model of simply supported symmetrically laid orthotropic rectangular composite laminated plate on four sides

$$\ddot{w}_1 + \omega_1^2 w_1 - \mu_1 \dot{w}_1 - \alpha_1 w_1^2 w_2 - \alpha_2 w_2^2 w_1$$

$$-\alpha_3 w_1^3 - \alpha_4 w_2^3 = F_1 \cos \Omega t \,, \qquad (1)$$

$$\ddot{w}_2+\omega_2^2 w_2-\mu_2\dot{w}_2-\beta_1 w_2^2 w_1-\beta_2 w_1^2 w_2$$
$$-\beta_3 w_2^3-\beta_4 w_1^3=F_2\cos\Omega t\,, \qquad (2)$$

where ω_1^2, β_1, β_2, β_3, β_4, F_2, ω_2^2, α_1, α_2, α_3, α_4, F_1 are constants associated with the system.

The main focus of this paper is to study the global bifurcation and chaotic dynamics of orthotropic composite laminated rectangular plates with symmetric layout, which are located on four simply supported sides. In order to ensure that the theoretical analysis results are more consistent with the dynamic characteristics of simply supported orthotropic composite laminated rectangular plates laid symmetrically on four sides, the equivalent coordinate transformation is introduced through the application of the coordinate transformation theory. The two degrees of freedom nonlinear ordinary differential equations for the first-order and second-order modes of symmetrically laid orthotropic composite laminated rectangular plates with four simply supported sides are rewritten as the differential control equations in the five dimensional phase space. Introduce the following coordinate transformation.

$$w_1=x_1,\ \dot{w}_1=x_2,\ w_2=x_3,\ \dot{w}_2=\omega_2 x_4,$$
$$\varphi=\Omega t\,, \qquad (3)$$

then, the equivalent form of system (1)-(2) can be represented as

$$\dot{x}_1=x_2\,, \qquad (4)$$

$$\dot{x}_2=-\omega_1^2 x_1+\alpha_1 x_1^2 x_3+\alpha_2 x_1 x_3^2+\alpha_3 x_1^3$$
$$+\alpha_4 x_3^3+\mu_1 x_2+F_1\cos\varphi \qquad (5)$$

$$\dot{x}_3=\omega_2 x_4\,, \qquad (6)$$

$$\dot{x}_4=-\omega_2^2 x_3+\frac{\beta_1}{\omega_2}x_1 x_3^2+\frac{\beta_2}{\omega_2}x_1^2 x_3$$
$$+\frac{\beta_3}{\omega_2}x_3^3+\frac{\beta_4}{\omega_2}x_1^3+\mu_2 x_4+\frac{F_2}{\omega_2}\cos\varphi\,, \qquad (7)$$

$$\dot{\varphi}=\Omega\,. \qquad (8)$$

The global dynamics of simply supported orthotropic laminated rectangular composite plates laid symmetrically on four sides were analysed.

Consider the following undisturbed system

$$\dot{x}_1=x_2\,, \qquad (9)$$

$$\dot{x}_2=-\alpha_1 x_1^2+\alpha_2 x_1 x_3^2+\alpha_3 x_1^3+\alpha_4 x_3^3\,, \qquad (10)$$

$$\dot{x}_3=\omega_2 x_4\,, \qquad (11)$$

$$\dot{x}_4=-\omega_2 x_3+\frac{\beta_1}{\omega_2}x_1 x_3^2+\frac{\beta_2}{\omega_2}x_1^2 x_3$$
$$+\frac{\beta_3}{\omega_2}x_2^3+\frac{\beta_4}{\omega_2}x_1^3\,, \qquad (12)$$

$(x_1,x_2,x_3,x_4)=(0,0,0,0)$ is the balance point in the unperturbed system, and the Jacobi matrix at this point is

$$A=\begin{bmatrix}0&1&0&0\\0&0&0&0\\0&0&0&\omega_2\\0&0&-\omega_2&0\end{bmatrix}. \qquad (13)$$

According to the characteristic equation at point (0,0,0,0,), the undisturbed system has a pair of eigenvalues with double zeros and a pair of eigenvalues with purely imaginary values, which are $\lambda_{1,2}=0$, $\lambda_{3,4}=\pm i\omega_2$, respectively.

The third order normal-form equations for the unperturbed system can be gained by using Maple program.

$$\dot{x}_1=x_2\,, \qquad (14)$$

$$\dot{x}_2=-\frac{1}{2}\alpha_2 x_1(x_3^2+x_4^2)-\alpha_3 x_1^3\,, \qquad (15)$$

$$\dot{x}_3=\omega_2 x_4+\frac{1}{2}\tilde{\beta}_2 x_1^2 x_4+\tilde{\beta}_3 x_4(x_3^2+x_4^2)\,, \qquad (16)$$

$$\dot{x}_4=-\omega_2 x_3-\tilde{\beta}_3 x_3(x_3^2+x_4^2)-\frac{\tilde{\beta}_2}{2}x_1^2 x_3\,, \qquad (17)$$

where $\tilde{\beta}_2=\dfrac{\beta_2}{\omega_2}, \tilde{\beta}_3=\dfrac{3\beta_3}{8\omega_2}$.

The equivalent coordinate transformation is performed by adding disturbance parameters to the damping and excitation of the equation

$$x_1=\sqrt{\frac{|\alpha_2|}{|\tilde{\beta}_2|}}u_1,\ x_2=\sqrt{\frac{|\alpha_2|}{|\tilde{\beta}_2|}}u_2,\ x_3=I\cos\gamma,$$

$$x_4=I\sin\gamma, \tag{18}$$

we get the system with perturbation parameters

$$\dot{u}_1=u_2, \tag{19}$$

$$\dot{u}_2=-\omega_1^2u_1+\frac{1}{2}\alpha_2I^2u_1+\tilde{\alpha}_3u_1^3+\mu_1u_2$$

$$+\tilde{F}_1\cos\Omega t, \tag{20}$$

$$\dot{I}=-\tilde{\mu}_2I\sin^2\gamma+\tilde{F}_2\sin\gamma\cos\Omega t, \tag{21}$$

$$I\dot{\gamma}=-\omega_2I+\tilde{\beta}_3I^3+\frac{1}{2}\alpha_2u_1^2I$$

$$+\tilde{\mu}_2I\sin\gamma\cos\gamma+\tilde{F}_2\cos\gamma\cos\Omega t, \tag{22}$$

$$\dot{\varphi}=\Omega, \tag{23}$$

Where $\tilde{\alpha}_3=\frac{\alpha_2\alpha_3}{\tilde{\beta}_2}$, $\tilde{F}_1=F\sqrt{\frac{|\tilde{\beta}_2|}{|\alpha_2|}}$, $\tilde{\mu}_2=\frac{\mu_2}{\omega_2}$, $\tilde{F}_2=\frac{F_2}{\omega_2}$.

The damping term and the excitation term are regarded as the perturbed term, and the following scaling is performed

$$\mu_1\to\varepsilon\mu_1,\tilde{\mu}_2\to\varepsilon\mu_2,F_1\to\varepsilon F_1,$$

$$\tilde{F}_2\to\varepsilon F_2, \tag{24}$$

and get the equation

$$\dot{u}_1=u_2, \tag{25}$$

$$\dot{u}_2=-\omega_1^2u_1+\frac{1}{2}\alpha_2u_1I^2+\tilde{\alpha}_3u_1^3$$

$$+\varepsilon\mu_1u_2+\varepsilon\tilde{F}_1\cos\varphi, \tag{26}$$

$$\dot{I}=-\varepsilon\tilde{\mu}_2I\sin^2\gamma+\varepsilon\tilde{F}_2\sin\gamma\cos\varphi \tag{27}$$

$$I\dot{\gamma}=-\omega_2I+\tilde{\beta}_3I^3+\frac{1}{2}\alpha_2u_1^2I$$

$$-\varepsilon\tilde{\mu}_2\sin\gamma\cos\gamma+\varepsilon\tilde{F}_2\cos\gamma\cos\varphi, \tag{28}$$

Let $\varepsilon=0$, then equations (25)-(27) can be rewritten as

$$\dot{u}_1=u_2, \tag{29}$$

$$\dot{u}_2=-\omega_1^2u_1+\frac{1}{2}\alpha_2u_1I^2+\tilde{\alpha}_3u_1^3, \tag{30}$$

$$\dot{I}=0, \tag{31}$$

$$I\dot{\gamma}=-\omega_2I+\tilde{\beta}_3I^3+\frac{1}{2}\alpha_2u_1^2I. \tag{32}$$

The Hamiltion function of an unperturbed system is

$$H=\frac{1}{2}u_2^2+\frac{1}{2}\omega_2^2u_1^2+\frac{1}{4}\alpha_2u_1^2I^2$$

$$+\frac{1}{4}\tilde{\alpha}_3u_1^4+\frac{1}{2}\omega_2I^2-\frac{1}{4}\tilde{\beta}_3I^4. \tag{33}$$

Since I=0, I appears as a parameter in space (u_1,u_2), the unperturbed system (29)-(32) is a decoupled two-degree-of-freedom system. We think about the two dimensional system of equations (29) and (30)

$$\dot{u}_1=u_2, \tag{34}$$

$$\dot{u}_2=-\omega_1^2u_1+\frac{1}{2}\alpha_2u_1I^2+\tilde{\alpha}_3u_1^3. \tag{35}$$

The forms of equations (34) and (35) for Hamilton function are as follows

$$H_0=\frac{1}{2}u_2^2+\frac{1}{2}Tu_1^2-\frac{1}{4}\tilde{\alpha}_3u_1^4, \tag{36}$$

where $T=-\frac{1}{2}\alpha_2I^2+\omega_1^2$.

We suppose equation (36) satisfy the conditions $T<0$, $\tilde{\alpha}_3<0$, $\alpha_2>0$. Let $\bar{T}=-T$, $\bar{\alpha}_3=-\tilde{\alpha}_3$, we get $I>\omega_1\sqrt{\frac{2}{\alpha_2}}$ or $I<-\omega_1\sqrt{\frac{2}{\alpha_2}}$ based on $\omega_1^2-\frac{1}{2}\alpha_2I^2<0$. The variables I and γ represent the nonlinear vibration amplitude and phase of equations (19)-(22), then $I\geq 0$, and the range of I satisfy $I>\omega_1\sqrt{\frac{2}{\alpha_2}}$. One can obtain system (33) has fixed points, and equilibrium point $(u_1,u_2)=\left(\pm\sqrt{\bar{T}/\tilde{\alpha}_3},0\right)$ are two stable center points, and equilibrium point (u_1,u_2)= (0,0) is a hyperbolic saddle point, where the

analytic expression of the homologous orbits linking the hyperbolic saddle point $(u_1, u_2) = (0,0)$ can be written as

$$u_1^h = \pm\sqrt{\frac{2\bar{T}}{\tilde{\alpha}_3}}\,\mathrm{sech}\sqrt{\bar{T}}\,t\,, \tag{37}$$

$$u_2^h = \mp\sqrt{\frac{2}{\tilde{\alpha}_3}}\bar{T}\,\mathrm{sech}\sqrt{\bar{T}}\,t\tanh\sqrt{\bar{T}}\,t\,. \tag{38}$$

Based on the hypothesis, we get

$$-\omega_2 I + \tilde{\beta}_3 I^3 + \frac{1}{2}\alpha_2 u_1^2 I = 0\,. \tag{39}$$

Let $u_1 = 0$, one get the resonance value $I_r = \sqrt{\frac{\omega_2}{\tilde{\beta}_3}}$.

On the basis of condition $I > \omega_1\sqrt{\frac{2}{\alpha_2}}$, the following inequality $\sqrt{\frac{\omega_2}{\tilde{\beta}_3}} > \omega_1\sqrt{\frac{2}{\alpha_2}}$ can be obtain, that is $\omega_2\alpha_2 > 2\tilde{\beta}_3\omega_1^2$. According to the former analysis, system parameters of equations (25)-(28) satisfy $\tilde{\alpha}_3 < 0$, $\alpha_2 > 0, \tilde{\beta}_3 > 0$, $\omega_2\alpha_2 > 2\tilde{\beta}_3\omega_1^2$.

Equation (37) is substituted into equation (32), and by integrating to get

$$\gamma(t) = \int_{t_0}^{t}\left(-\omega_2 + \tilde{\beta}_3 I^2 + \frac{1}{2}\alpha_2 u_1^2\right)dt$$

$$= -\frac{2\alpha_2}{\tilde{\alpha}_3}\sqrt{\bar{T}}\tanh\sqrt{\bar{T}}\,t + \gamma_0\,. \tag{40}$$

As

$$\Delta\gamma(I_\gamma) = \int_{-\infty}^{+\infty}\Omega\left(x^h(\tau, I_\gamma)I_\gamma\right)d\tau\,,$$

we obtain

$$\Delta\gamma = \int_{-\infty}^{+\infty} -\frac{1}{2}\alpha_2 u_1^2\,dt$$

$$= \frac{\alpha_2}{\tilde{\alpha}_3}\sqrt{\bar{T}}\int_{-\infty}^{+\infty}\mathrm{sech}^2\sqrt{\bar{T}}\,t\,dt$$

$$= -\frac{2\alpha_2}{\tilde{\alpha}_3}\sqrt{\bar{T}}\,. \tag{41}$$

As $M(I_\gamma, \gamma_0, \varphi_0, \mu) = \int_{-\infty}^{+\infty}\left\langle n(p^h(t)), g(p^h(t)), \omega t + \varphi_0, \mu, 0\right\rangle$ the Melnikov function of equations (25)-(28) is

$$M = \int_{-\infty}^{+\infty}[-\mu_1 u_2^2 + u_2\tilde{F}_1\cos(\Omega t + \varphi_0)$$

$$+\frac{1}{2}\alpha_2\mu_1^2 I_0(\tilde{\mu}_2 I_0\sin\gamma\cos(\Omega t + \varphi_0))]dt$$

$$-\frac{4\mu_1\bar{T}^{\frac{3}{2}}\pi}{3\tilde{\alpha}_3} - \sqrt{\frac{2\bar{T}}{\tilde{\alpha}_3}}\pi\Omega\tilde{F}_1\sin\varphi_0\,\mathrm{sech}\frac{\Omega\pi}{2\sqrt{\bar{T}}}$$

$$\int_{-\infty}^{+\infty}\frac{1}{2}\alpha_2 u_1^2 I_0(-\tilde{F}_2\sin\gamma\cos(\Omega t + \varphi_0))dt$$

$$-\frac{1}{2}\tilde{\mu}_2 I_0^2\left(\Delta\gamma - \sin\Delta\gamma\right). \tag{42}$$

Through calculation, the single pulse Melnikov function of equations (25)-(28) is

$$M_1 = -\frac{4\mu_1\bar{T}^{\frac{3}{2}}\pi}{3\tilde{\alpha}_3} - \pi I_0\tilde{F}_2\,\mathrm{csch}\frac{\Omega\pi}{2\sqrt{\bar{T}}}\sin\varphi_0$$

$$-\sqrt{\frac{2\bar{T}}{\tilde{\alpha}_3}}\pi\Omega\tilde{F}_1\sin\varphi_0\,\mathrm{sech}\frac{\Omega\pi}{2\sqrt{\bar{T}}}$$

$$-\frac{1}{2}\tilde{\mu}_2 I_0^2(\Delta\gamma - \sin\Delta\gamma)\,. \tag{43}$$

For the same reason, the systemic k- pulse Melnikov function is

$$M_k = -\frac{4\mu_1\bar{T}^{\frac{3}{2}}\pi}{3\tilde{\alpha}_3}k - k\pi I_0\tilde{F}_2\,\mathrm{csch}\frac{\Omega\pi}{2\sqrt{\bar{T}}}\sin\varphi_0$$

$$-k\sqrt{\frac{2\bar{T}}{\tilde{\alpha}_3}}\pi\Omega\tilde{F}_1\sin\varphi_0\,\mathrm{sech}\frac{\Omega\pi}{2\sqrt{\bar{T}}}$$

$$-\frac{1}{2}\tilde{\mu}_2 I_0^2(\Delta\gamma - \sin\Delta\gamma)\,. \tag{44}$$

Theorem 1 If the K-pulse Melnikov function exists a simple zero and its first derivative is not zero, the stable and unstable manifolds in the system will intersect each other transversally, indicating the occurrence of the multi-

pulse chaotic motion in the system (1)-(2) following the concept of Smale's horseshoe.

As $\operatorname{sech}\frac{\Omega\pi}{2\sqrt{\bar{T}}} \in (0,1]$,if $\frac{\Omega\pi}{2\sqrt{\bar{T}}} \geq \lg(\sqrt{2}+1) \approx 0.8814$, we have $\operatorname{csch}\frac{\Omega\pi}{2\sqrt{\bar{T}}} \leq 1$; if $0 < \frac{\Omega\pi}{2\sqrt{\bar{T}}} < \lg(\sqrt{2}+1)$, we have $\operatorname{csch}\frac{\Omega\pi}{2\sqrt{\bar{T}}} > 1$, Therefore, it is probable to find appropriate parameters that meet theorem 1, as a result, system (1)-(2) will exhibit multi-pulse chaotic motion in the sense of Smale's horseshoe.

3. THEORETICAL ANALYSIS

According to the above-mentioned theoretical derivation so as to gain that $\tilde{\alpha}_3 < 0$, $\alpha_2 > 0$, $\tilde{\beta}_3 < 0$. Now take the parameters $\mu_1 = -0.78$, $\mu_2 = 0.16$, $\omega_1 = 2.2$, $\alpha_1 = -23$, $\alpha_2 = 3.9$, $\alpha_3 = -10.8$, $\alpha_4 = -3.7$, $\omega_2 = -2.6$, $\beta_1 = -4.2$, $\beta_2 = 16.8$, $\beta_3 = -13.6$, $\beta_4 = -3.2$, $\Omega_1 = 1$, $\Omega_2 = 1$, and initial values are $x_1 = 0.8913$, $x_2 = 0.7621$, $x_3 = 0.4565$, $x_4 = 0.0185$.

Fig. 2 shows a two-dimensional bifurcation diagram of a composite laminated rectangular plate system that is simply supported and orthotropic with symmetrically laid layers. Fig. 2(a) displays the bifurcation diagram in phase space (F_1, x_1) and the bifurcation diagram in phase space (F_1, x_3) is shown in Fig. 2(b).

The amplitude of external excitation F_1 is represented on the horizontal axis, and the displacement of the first-order and second-order modes of orthotropic symmetrical composite rectangular laminates on four simply supported sides is represented on the vertical axis, respectively.

Fig. 2 can visually demonstrate the multi-pulse chaotic motion for the orthotropic composite lamellar rectangular plate system with simply supported symmetric laying on four sides under the action of external excitation F_1.

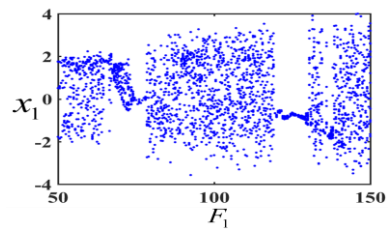

(a) Bifurcation diagram of first-order mode

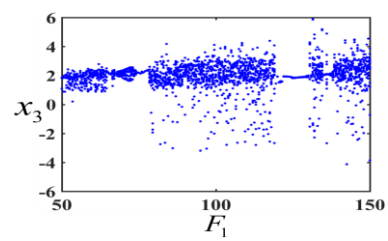

(b) Bifurcation diagram of second-order mode

Figure 2 Bifurcation diagram of orthotropic symmetrically laid composite laminated rectangular plate

As shown in Fig. 2, when the external excitation amplitude F_1 of the four-sided simply supported orthotropic sympathetically laid composite laminated rectangular plate increases from 50 to 150, the system undergoes a transformational process from chaotic motion to periodic motion and back to chaotic motion. It can be observed from Fig. 2(a) that the vibration response of the first-order mode of the four-sided simply supported symmetrically laid orthotropic composite rectangular laminated plate exhibits chaotic operation. The system exhibits a period-doubling motion with increase of the amplitude under the external excitation. With further increase in the amplitude of the external excitation, the vibration response of the system transitions from chaotic motion to periodic motion and then back to chaotic motion; It is evident to find from Fig. 2(b) that the vibration response of the second-order mode of the four-sided simply supported symmetrically laid orthotropic composite rectangular laminated plate is similar to that of the first-order mode, and the vibration response generated by the system also alternates between chaotic motion and periodic motion. By comparing Fig. 2(a) and Fig. 2(b), it is evident that the first-order mode of vibration for the

four-sided simply supported symmetrically laid orthotropic composite laminated rectangular plate has a smaller amplitude than the second-order mode.

Fig. 3 represents the maximum Lyapunov exponent diagram of the four-sided simply supported orthotropic symmetrically laid composite laminated rectangular plates system. It is evident from the Fig. 3 that the interval of chaotic motion in the system in accordance with that of chaotic motion in the bifurcation diagram Fig. 2.

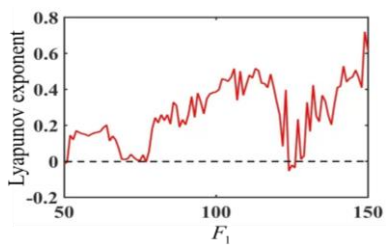

Figure 3 Lyapunov diagram of orthotropic symmetrically laid composite laminated rectangular plate

The external excitation amplitude $F_1 = 60$ is taken, and it can be judged from Fig. 2 and Fig. 3 that chaotic motion occurs in system (1)-(2). Next, the chaotic motion of the system subjected to the action of additional excitation is further verified through phase diagram and time history diagram. Figure 4 shows that chaos occurred in the system of composite laminated rectangular plates laid symmetrically on four sides simply supported orthotropic when the external excitation amplitude $F_1 = 60$. Fig. 4(a) is the phase diagram in plane (x_1, x_2), Fig. 4(b) is the time history diagram in plane (t, x_1), Fig. 4(c) is the phase diagram in plane (x_3, x_4), and Fig. 4(d) shows the temporal course diagram in plane (t, x_3).

As depicted in Fig. 4(a) and 4(b), the vibration response of the first-order mode of the orthotropic laid symmetrically composite laminated rectangular plate system on four simply supported sides exhibits chaotic motion, and there is a chaotic attractor located at the origin of the system. Fig. 4(c) and 4(d) show that the vibration response of the orthotropic symmetrically laid composite laminated rectangular plate system with four simply supported sides also exhibits chaotic motion for the second order mode, and the system displays chaotic attractors on both sides of the origin.

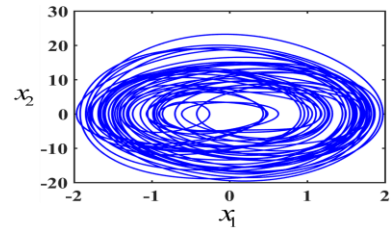

(a) The phase portrait on plane (x_1, x_2)

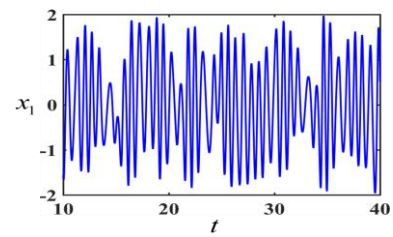

(b) The time history portrait on plane (t, x_1)

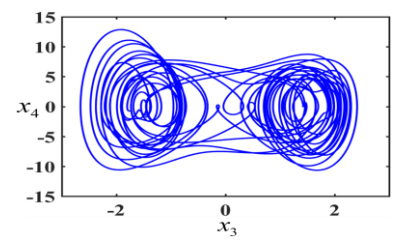

(c) The phase portrait on plane (x_3, x_4)

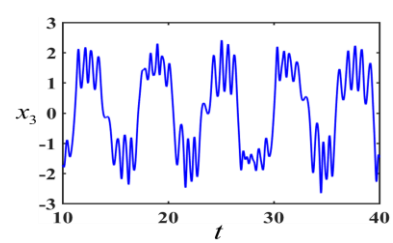

(d) The time history portrait on plane (t, x_3)

Figure 4 Chaotic motion of simply supported orthotropic symmetrically laid composite laminated rectangular plate on four sides at the external excitation F_1=60

In Fig. 5 and Fig. 6, when F_1=120 and F_1=140, chaos occur in the system of rectangular composite laminated rectangular plates laid symmetrically with simply supported orthotropic materials on four sides. It is easy to notice that the number of chaotic attractors in the first and second order modes of the simply supported orthotropic symmetrically laid composite laminated rectangular plate system on four sides remains unchanged with the increase in the amplitude of external excitation. On the basis of Fig. 5(d) and Fig. 6(d), the corresponding amplitude of

vibration for the second order mode of the simply supported orthotropic symmetrically laid rectangular composite laminated plate system varies under different external excitation.

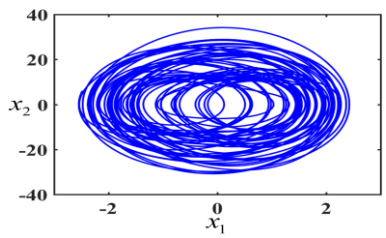

(a) The phase portrait on plane (x_1, x_2)

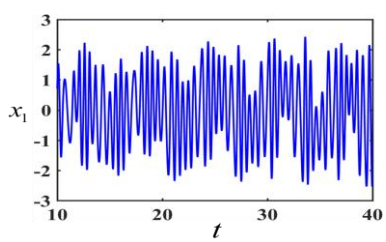

(b) The time history portrait on plane (t, x_1)

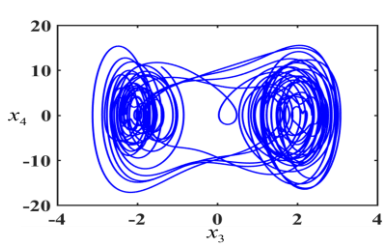

(c) The phase portrait on plane (x_3, x_4)

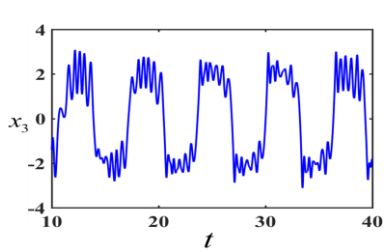

(d) The time history portrait on plane (t, x_3)

Figure 5 Chaotic motion of simply supported orthotropic symmetrically laid composite laminated rectangular plate on four sides at the external excitation F_1=120

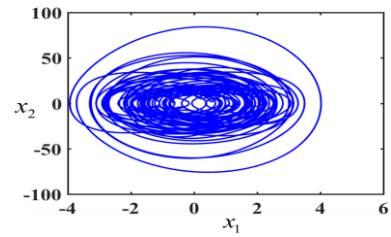

(a)The phase portrait on plane (x_1, x_2)

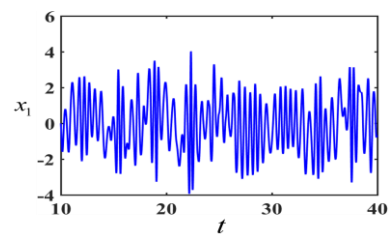

(b) The time history portrait on plane (t, x_1)

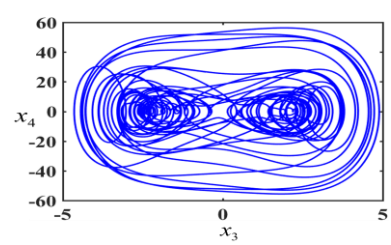

(c) The phase portrait on plane (x_3, x_4)

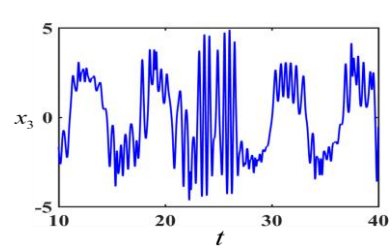

(d) The time history portrait on plane (t, x_3)

Figure 6 Chaotic motion of simply supported orthotropic symmetrically laid composite laminated rectangular plate on four sides at the external excitation F_1=140

4. CONCLUSION

This paper explores the global bifurcation and chaotic dynamics of orthotropic symmetrically laid rectangular composite laminated plates with four simply supported sides under the external excitation F_1. The utilization of the coordinate transformation theory leads to the derivation of the five-dimensional dynamic system in composite laminated rectangular plates. The nonlinear term that has a relatively small impact on the global

dynamics of the system is determined using the canonical form theory. The system is reduced to the sum of the undisturbed part and the disturbed part. The k-pulse Melnikov function, used to assess the occurrence of the multi-pulse chaotic motion in the system, is calculated by using the generalized Melnikov theorem. The study determine the chaotic threshold interval for the rectangular plate made of four-sided simply supported orthotropic symmetrically laid composite laminates. Through theoretical analysis and numerical simulation, the multi-pulse chaotic motion in the rectangular plate system with composite material lamination in the sense of Smale's horseshoe is further verified. The conclusions are as follows:

(1) Both the bifurcation diagram and the maximum Lyapunov exponential diagram verify that multi-pulse chaotic motion will occur in the system, and the regions of chaotic motion identified in the bifurcation diagram and the maximum Lyapunov exponential diagram are consistent. The bifurcation diagram reveals that as the amplitude of the external excitation increases, the system can go through various vibration states, such as quasi-periodic, periodic and chaotic motion.

(2) From Fig. 4 to 6, it can be observed that there is an chaotic attractor in the systemic first order mode, while there are two chaotic attractors in the systemic second order mode. Additionally, as the amplitude increases in the excitation, the chaotic attractor region of the system expands correspondingly.

(3) It can be observed from the time history diagrams in Fig. 5 and Fig. 6 that with the increment of excitation amplitude, the amplitudes in vibration with both the first-order and second-order modes in the system also experience an increase. Therefore, the amplitudes of the orthotropic symmetrically laid composite laminated rectangular plates on four simply supported sides can be controlled by adjusting the amplitude of the external excitation.

REFERENCES

[1] H. S. Shen, Y. Xiang and F. Lin. Thermal buckling and postbuckling of functionally graded grapheme reinforced composite laminated plates resting on elastic foundations. Thin Wall Struct., 118 (2017), pp. 229-237. http://dx.doi.org/10.1016/j.matdes.2017.07.025

[2] S. Atobe, S. Nonami, N. Hu and H. Fukunaga. Identification of impact force acting on composite laminated plates using the radiated sound measured with microphones. J. Sound Vib., 405 (2017), pp. 251-268. https://doi.org/10.1016/j.jsv.2017.06.009

[3] Y. S. Joshana, N. Grovera and B. N. Singh. Analytical modelling for thermo-mechanical analysis of cross-ply and angle-ply laminated composite plates. Aerosp. Sci. Technol., 70 (2017), pp. 137-151. https://doi.org/10.1016/j.ast.2017.07.041

[4] W. Zhang, S. F. Lu and X. D. Yang. Analysis on nonlinear dynamics of a deploying composite laminated cantilever plate. Nonlinear Dynam., 76 (2014), pp. 69-93. https://schlr.cnki.net/Detail/doi/GARJ2014/SSJD14041100000849

[5] S. W. Yang, W. Zhang, Y. X. Hao and Y. Niu. Nonlinear vibrations of FGM truncated conical shell under aerodynamics and in-plane force along meridian near internal resonances. Thin wall Struct., 42 (2019), pp. 369-391. https://doi.org/10.1016/j.tws.2019.04.024

[6] T. Ma, X. J. Song and S. F. Lv. Nonlinear dynamics modeling and subharmonic resonances analysis of a laminated composite plate. Sound Vib., 2020 (2020), pp. 7913565. https://doi.org/10.1155/2020/7913565

[7] S. W. Yang, Y. X. Hao, W. Zhang, L. Yang and L. T. Liu. Buckling and free vibration of eccentric rotating CFRP cylindrical shell base on FSDT. Appl. Math. Model., 95 (2021), pp. 591-611. https://doi.org/10.1016/j.apm.2021.02.029

[8] S. W. Yang, Y. X. Hao, W. Zhang, L. Yang and L. T. Liu. Free vibration and buckling of eccentric rotating FG-GPLRC cylindrical shell using first-order shear deformation theory. Compos. Struct., 263 (2021), pp. 113728. https://doi.org/10.1016/j.compstruct.2021.113728

[9] M. Q, Wu, W, Zhang and Y. Niu. Experimental and numerical studies on nonlinear vibrations and dynamic snap-through phenomena of bistable asymmetric composite laminated shallow shell under center foundation excitation. Eur. J. Mech. A-Solid, 89 (2021), pp. 104303. https://doi.org/10.1016/j.euromechsol.2021.104303

[10] M. Noroozi and F. Bakhtiari-Nejad. Nonlinear vibration of a nanocomposite laminated piezoelectric trapezoidal actuator in subsonic airflow under combined electrical and forcing excitations. P. I. Mech. Eng. C-J Mec., 235 (2020), pp. 4784-4817. https://doi.org/10.1177/0954406220911075

[11] W, Zhang, J. H Zhang. Chaotic dynamics of non-autonomous composite laminates. Chinese Quarterly

of Mechanics. 2009, 30(1): 127-132.

[12] W. Zhang, M. H. Zhao and X. Y. Guo. Nonlinear responses of a symmetric cross-ply composite laminated cantilever rectangular plate under in-plane and moment excitations. Compos. Struct., 100 (2013), pp. 554-565. https://doi.org/10.1016/j.compstruct.2013.01.013

[13] S. T. Zhu, J. Li and W. Zhang. Study on multi-period motion of negative Poisson's ratio honeycomb sandwich panel. Journal of Dynamics and Control, 19 (2021), pp. 33-38.

[14] W. S. Ma, S. F. Lu, S. W. Yang and W. Zhang. Study on complex dynamics of circular antenna structure. Journal of Dynamics and Control, 20 (2022), pp. 40-49.

[15] K. Yagasaki. The method of Melnikov for perturbations of multi-degree-of-freedom Hamiltonian systems. Nonlinearity, 12 (1999), pp. 799-822. https://doi.org/10.1088/0951-7715/12/4/3043